



DNase-I functionalization of ciprofloxacin-loaded chitosan nanoparticles overcomes the biofilm-mediated resistance of *Pseudomonas aeruginosa*

Krishna Kumar Patel¹ · Ashish Kumar Agrawal¹ · Md. Meraj Anjum¹ · Muktanand Tripathi² · Nidhi Pandey² · Sankha Bhattacharya¹ · Ragini Tilak² · Sanjay Singh¹

Received: 12 June 2019 / Accepted: 5 August 2019 / Published online: 16 August 2019
© King Abdulaziz City for Science and Technology 2019

Abstract

Pseudomonas aeruginosa infection in cystic fibrosis (CF) is a major complication which aggravates the disease complexity and progression. The improvement of antimicrobial therapy against the *P. aeruginosa* biofilm infection in CF by disseminating the extracellular matrix is a fundamental concept of this study. Chitosan nanoparticle was successfully fabricated and characterized. Furthermore, various in vitro antimicrobial efficacy, biofilm dispersal potential, and in vitro as well as in vivo toxicity were assessed. The chitosan nanoparticles of ciprofloxacin functionalized with DNase-I had spherical shape with desired quality attributes (particle size— 212.3 ± 8.9 ; polydispersity index— 0.288 ± 0.06 , zeta potential— 14.6 ± 1.3 , and entrapment efficiency— $53.7 \pm 3.8\%$). The developed DNase-I functionalized chitosan nanoparticles laden with ciprofloxacin demonstrated substantial and prolonged microbial inhibition, efficiently prevented the biofilm development, and possessed the excellent biofilm dispersal potential. Moreover, the confocal study demonstrated that the biofilm treated with DNase-I functionalized chitosan nanoparticles of ciprofloxacin had minimum biofilm thickness, biomass, and microbial density compared to the other treatment groups. Additionally, the developed formulation was found to be safe and had minimal in vitro as well as in vivo toxicity. Thus, the findings of this study suggests ciprofloxacin-loaded chitosan nanoparticles functionalized with DNase-I as an effective and safe treatment approach for the *P. aeruginosa* infection in CF.

Keywords Chitosan nanoparticles · DNase-I · Cystic fibrosis · Ciprofloxacin · Biofilm

Introduction

Pseudomonas aeruginosa, an omnipresent, opportunistic, and highly heterogeneous gram-negative bacterium with different phenotypes, is a major reason for nosocomial infection (Pang et al. 2019). Persistent *P. aeruginosa* infection in cystic fibrosis (CF) in association with inherent complication of CF including chronic pulmonary inflammation and progressive impairment to the pulmonary

function is an underlying reason of morbidity and mortality. Mostly, it is associated with copious biofilm formation in the CF patient's lung and inflicts bigger obstacle to the antibiotic therapy. Moreover, the ability to adopt different phenotypes either as non-mucoid (non-alginate producing strain) or mucoid (hyper alginate producing strain) during biofilm production makes the *P. aeruginosa* infection more resistant to the antibiotic therapy (Oliver et al. 2000; Sauer et al. 2002; Kidd et al. 2018). Biofilms facilitated bacterial infection, a physical modification in the living environment, has been accepted as most frequent and aggressive mechanism of resistance. Biofilm is a highly antibiotic and immune-resistant surface attached (biotic or abiotic) well-organized consortium of microbial colonies, which confined within the dense architecture of self-secreted extracellular matrix (ECM). Consequently, antibiotics fails to produce the sufficient concentration (minimum inhibitory concentration) needed in close vicinity of microbial

✉ Ashish Kumar Agrawal
ashish.phe@iitbhu.ac.in

✉ Sanjay Singh
ssingh.phe@iitbhu.ac.in

¹ Department of Pharmaceutical Engineering and Technology, Indian Institute of Technology (IIT-BHU), Varanasi, India

² Department of Microbiology, Institute of Medical Sciences, Banaras Hindu University, Varanasi, India

colonies surrounded by ECM (Del Pozo and Patel 2007; Rybtke et al. 2011; Pang et al. 2019).

Predominantly, extracellular DNA is a substantial constituent in the ECM of non-mucoid strain of *P. aeruginosa* in contrast to mucoid strains (abundantly secrete alginate) as a result of quorum sensing which further initiates the secretion of extracellular DNA by autolysis of cell. Extracellular DNA magnifies the diseased condition by facilitating cell-to-cell connectivity and cell-to-biofilm connectivity in conjunction with stimulating cell surface adhesion, cell accumulation, biofilm progression, biofilm establishment, inflexibility, and providing the three-dimensional structure. Simultaneously, being negatively charged it averts the penetration of positively charged antibiotics (e.g., aminoglycosides) due to electrostatic interaction, thereby reducing the bacterial susceptibility (Whitchurch et al. 2002; Chiang et al. 2013). Hence, the biofilm imposes the major hurdle to the antimicrobial therapy by hampering the drug diffusion in biofilm, binding and repelling electrostatically to charged antibiotics, and escaping the innate immunity of host.

Even though several strategies including, quorum sensing quenching agents (RNAIII-inhibiting peptide); biofilm dispersal by modifying the c-di-GMP target; bacterial amyloid inhibition; and use of various nanoparticles (polymeric or lipid) have been investigated concurrently with antibiotic to actively eliminate the biofilm, an unmet need is still persisting (Cutting et al. 2009; Wu et al. 2015; Algburi et al. 2017).

Nanoparticles (NPs), being in submicron range, offer controlled drug release, higher drug stability against adverse biofilm environment, and higher penetration in the biofilm, and can effectively deliver the drug in the close proximity of microbial colonies. In fact, NPs have been proved to have improved antibiotics susceptibility against biofilm embedded bacterial colonies and has the potential to avoid the bacterial tolerance alongside the therapy. Moreover, it offers the easy surface modification with the certain targeting moieties (including protein and peptides) due to high surface area and incorporated functional group (Forier et al. 2014; Ramos et al. 2018).

The current hypothesis attempted to formulate the DNase-I functionalized chitosan nanoparticles of ciprofloxacin to competently eliminate *P. aeruginosa* infection in the CF patients by averting the microbial resistance. The selection of chitosan is based on the earlier reports in which chitosan itself has been reported to have antimicrobial properties, while the selection of DNase-I as targeting ligand is based on its potential to disrupt the biofilm's extracellular DNA that have the fundamental role in biofilm generation, dispersal, and disease progression (Alipour et al. 2009; Okshevsky et al. 2015; Juárez-Morales et al. 2017).

Materials and methods

Materials

Ciprofloxacin was a liberal gift by Cadila Healthcare Ltd., Ahmadabad (India). Deoxyribose nuclease I (DNase-I) and Chitosan (140KD MW; $\geq 75\%$ deacetylated, catalogue no. 42344) were procured from Sigma-Aldrich, Bangalore (India). Similarly, SYTO9/propidium iodide (live/dead cell recoloring pack) was obtained from Thermo Fischer Scientific, India. In addition, the other compounds, solvents, and reagents, of analytical grade were purchased from different vendors.

Preparation of chitosan nanoparticles and functionalization with DNase-I

Tripolyphosphate (TPP) cross-linked chitosan nanoparticles loaded with ciprofloxacin (CIP-CHNPs) were formulated by ionotropic gelation process (Harde et al. 2014; Agrawal et al. 2015; Urimi et al. 2019). Briefly, 0.2% w/v chitosan was dissolved in 0.1% v/v acetic acid and further supplemented with ciprofloxacin in the subsequent step (20% w/w of chitosan). After adjusting the chitosan solution pH to 6.0–6.5 by 1 N NaOH, 0.1% w/v TPP (1:4 ratio with chitosan) was added gradually with continuous stirring (1200 rpm) to form ciprofloxacin-loaded cross-linked chitosan nanoparticle (CIP-CHNPs).

The optimized CIP-CHNPs were further mixed with DNase-I (100 $\mu\text{g}/\text{ml}$) in the presence of EDAC and NHS solution (0.1 M each for 30 min) to form the covalent bond (amide) among the free amino groups on the chitosan and carboxylic group of DNase-I. The DNase-I functionalized chitosan nanoparticles of ciprofloxacin (DNase-CIP-CHNPs) were eventually recovered by centrifuging the reaction mixture at 1600g for 20 min in centrifuge tube on 20 μl glycerol bed and washed gently using distilled water.

Preparation of freeze-dried inhalable powder

Freeze drying process was used to make the dried powder of NPs (Agrawal et al. 2013; Harde et al. 2014). Briefly, drying process started with pre-freezing at $-40\text{ }^\circ\text{C}$ for 1 h and then subjected to first step drying at $-20\text{ }^\circ\text{C}$ for 24 h. Eventually, secondary drying at $20\text{ }^\circ\text{C}$ was carried out for 24 h at 1 Pa pressure. Furthermore, as the particle less than 1 μm in size easily exhaled from the lungs, and hence, it should have the particles size in the range of 2–5 μm . Therefore, to attain the mass median aerodynamic diameter (MMAD), apposite for inhalation, and improve the stability of NPs keeping all the unique characteristics unaffected, freeze-dried

DNase-CIP-CHNPs were permitted to settle (adsorb) on the fine lactose powder surface (InhaLac-500, Meggle). Concisely, the freeze-dried NPs and lactose in the ratio 90:10 were vortexed at $50 \pm 5\%$ relative humidity. Finally, the flow property in terms of angle of repose was measured.

DNase-I conjugation confirmation

Ninhydrin method was modified to some extent for quantitative identification of DNase-I conjugation with CIP-CHNPs obtained after carbodiimide reaction (Prochazkova et al. 1999). Briefly, after necessary ninhydrin reaction of 50 $\mu\text{g}/\text{ml}$ CIP-CHNPs and DNase-CIP-CHNPs test samples, absorbance at 570 nm (A_{570}) was measured to calculate the % free amino group by the following formula:

$$\% \text{ Free amino group} = \frac{(A_{570} \text{ DNase-CIP-CHNPs})}{A_{570} \text{ CIP-CHNPs}} \times 100.$$

DNase-I activity assay

DNA plasmid dissolved in 6.25 mM magnesium sulfate to produce 50 $\mu\text{g}/\text{ml}$ concentration then dilutes with 1 M acetate buffer (pH 5) and distilled water in 8:1:1 (MgSO_4 :acetate buffer:water) ratio. The DNA sample was filled in the 96-well plate and incubated with DNase-I and DNase-CIP-CHNPs at 25° for 30 min. Following the incubation, absorbance was measured at 260 nm using multi-mode plate reader, SYNERGY/HTX, Biotek. Finally, the % hydrolytic activity of DNase-I and DNase-CIP-CHNPs was calculated.

Particle size, polydispersity index, and zeta potential measurement

The method reported in the previous studies was performed to assess the particle size (PS), polydispersity index (PDI), and zeta potential (ZP) with the help of particle-size analyzer (DelsaNanoC, Beckman coulter, USA) (Agrawal et al. 2017a, b; Patel et al. 2019a). Exactly ten times diluted nanoparticle samples were filled in the cell specific to the PS and ZP analysis. Each analysis was performed thrice to get the statistically valid data.

% Entrapment efficiency (EE) assessment

CIP-CHNPs or DNase-CIP-CHNPs (500 μl) suspension was transferred above the micro filter of nanosep tube and centrifuged with the rotating speed of 1500 rpm for 10 min using the cooling centrifuge (REMI). Furthermore, the filtered sample collected down the filter in nanosep tube was diluted suitably and analyzed spectrophotometrically at 279 nm to

find out the %EE using the following formula (Jain et al. 2012; Kushwah et al. 2018):

$$\% \text{ EE} = \frac{\text{Total drug added initially} - \text{Free drug in suspension}}{\text{Total Drug added initially}} \times 100.$$

Scanning electron microscopy (SEM)

Surface characterization, such as shape, texture, and PS, of the optimized CIP-CHNPs and DNase-CIP-CHNPs was evaluated using SEM ZEISS, EVO18, Germany (scanning electron microscope). In brief, the surface-dried test sample on copper strip was coated with gold prior to the analysis to enhance the conductivity of particles surface and observed under SEM (Jain et al. 2015; Patel et al. 2019a).

In vitro aerodynamic properties of dry powder

Determination of aerodynamic properties in terms of mass median aerodynamic diameter (MMAD) and fine particle fraction (FPF) are the critical parameters to assess the expected fraction of particles to be deposited deep inside the lungs and achieve the desirable concentration. Eight-stage Andersen Cascade Impactor, having effective cut off diameter 9 μm (Stage 0), 5.8 μm (stage 1), 4.7 μm (stage 2), 3.3 μm (stage 3), 2.1 μm (stage 4), 1.1 μm (stage 5), 0.65 μm (stage 6), and 0.43 μm (stage 7), was used to determine the MMAD and FPF. The sequential process described in the previous publication was performed to obtain the desired responses. In the end, FPF and MMAD was figured out from the raw data obtained in the study (Yang et al. 2009).

P. aeruginosa strain and characterization

Strain of *P. aeruginosa*, isolated from clinical samples and after routine biochemical identification evaluation, was willingly provided by the Department of Microbiology, Institute of Medical Sciences, Banaras Hindu University, Varanasi, India. The selected strain was incubated overnight in Luria–Bertani medium at 37°C for complete growth and finally confirmed the growth by measuring the absorbance at λ_{max} 550 nm after centrifugation at 5000 rpm for 10 min.

Minimum inhibitory concentration (MIC)

Minimum inhibitory concentration of optimized DNase-CIP-CHNPs along with other treatment groups was evaluated by broth dilution method (Patel et al. 2019b). Concisely, 96-well plate preoccupied with 100 μl treatments groups with serial dilutions from 8, 4, 2, 1, 0.5, 0.25, 0.125, 0.0625, 0.0312, and 0.0156 $\mu\text{g}/\text{ml}$ was inoculated with 0.5×10^6 CFU/ml and stored at 37°C for 48 h for incubation. Subsequently, absorbance at 550 nm was recorded at successive

24 h and 48 h in the multi-mode plate reader, SYNERGY/HTX, Biotek.

Minimum biofilm inhibitory concentration

Minimum biofilm inhibitory concentration (MBIC) required for preventing the biofilm growth in planktonic culture of *P. aeruginosa* was assessed. The procedure similar to the MIC was followed to prepare the test 96-well plate except prior to incubation the plate was covered with lid having the 96 peg to provide the surface for bacterial attachment and biofilm growth. The prepared plates were stored at 37 °C for 48 h on the rotary shaker. After the successive interval of 24 h and 48 h, the covered peg lid was washed to remove the loosely attached *P. aeruginosa* cell and ultrasonicated to collect the biofilm producing cell from peg in fresh 96-well plate containing the 200 µl LB. Finally, the collected cells were inoculated on solid agar plates to visualize and count the colony forming units (CFU) after 24 and 48 h.

Minimum biofilm eradication concentration (MBEC)

Precisely, biofilm was developed (using 0.5×10^6 CFU/ml *P. aeruginosa* inoculated in 200 µl LB) on the peg lid in sterile, transparent polystyrene 96-well culture plate (BRAND plates) during 48 h incubation. Subsequently, the lightly adhered planktonic cells were detached from biofilm by washing with PBS. The peg lid containing the biofilm was covered on the 96-well plate containing the test samples (CIP, CIP + DNase-I, CIP-CHNPs, CIP-CHNPs + DNase-I, and DNase-CIP-CHNPs) diluted with LB to produce the concentration 8, 4, 2, 1, 0.5, 0.25, 0.125, 0.0625, 0.0312, and 0.0156 µg/ml equivalent to CIP. After 24 h incubation at 37 °C, the treated peg lids were covered over the fresh 96-well plate preoccupied with freshly prepared LB medium and dispersed the residues of biofilm by sonication. Eventually, the bacterial cell recovered after sonication was cultured over LB agar medium to determine the remaining CFU in biofilm and calculate the % biofilm remaining (Baelo et al. 2015).

Repeated dose elimination of biofilm

The biofilm grown during 48 h on peg lid as per the MBEC study was treated three successive doses once a day at MIC (0.187 µg/ml) to find out the relative efficacy of DNase-CIP-CHNPs with CIP and other related formulation in terms of biofilm eradication potential. The % residue was calculated (CFU) as per the details given above in MBIC/MBEC studies.

Confocal microscopic evaluation of established biofilm

The biofilm was grown on coverslip in 12-well culture plate as per the procedure described above. Subsequently after incubation with NPs and CIP (0.187 µg/ml) for 24 and 48 h, grown *P. aeruginosa* biofilm was fixed with 4% w/v paraformaldehyde on the coverslip and stained with 6 µM SYTO 9/30 µM propidium iodide mixture (LIVE/DEAD BacLight kit; Thermo Fischer, India).

Stained biofilm smears were visualized under confocal laser scanning microscope (CLSM, ZEISS, Germany) to obtain the fluorescent images of biofilm. Using the 40× magnifications and 488 nm and 560 nm excitation, the smears' Z-stack images were captured at 2.03 µm step size. Finally, the fluorescent z-stack images were quantitatively analyzed using the COMSTAT 2 to determine the biofilm thickness and biomass for each treatment group (Mu et al. 2016).

MTT assay

In vitro cytotoxicity of DNase-CIP-CHNPs against lungs epithelium cell (BEAS-2B, ATCC) was evaluated by 3-[4,5-dimethylthiazol-2-yl]-2,5-diphenyltetrazolium bromide (MTT) test by following the previously reported protocol (Aqil et al. 2017; Kushwah et al. 2017). Briefly, cell line was incubated with different formulation to check the probable toxicity and the results in terms of percentage cell viability were plotted.

In vivo toxicity study

In vivo toxicity was evaluated by exposing the lungs of Wistar rats weighing 200–250 g to newly formed formulation and other components. Five test groups each having three animals including the control, CIP, CIP + DNase-I, CIP-CHNPs, CIP-CHNPs + DNase-I, and DNase-CIP-CHNPs were tested for in vivo study. The Central Animal Ethical Committee, Faculty of Medicine, Institute of Medical Sciences, Banaras Hindu University permitted the specified procedure for in vivo toxicity evaluation.

Precisely, 100 mg powdered formulation, kept on centrifugal tube cap (15 ml volume) of in-house developed apparatus, was aerosolized by flowing the pressurized air from the orifice provided at the tip of tube using actuating rubber pipette bulb (Muttill et al. 2007). Simultaneously, the rat's nostrils were popped in the orifice for 30 s to breath in the powdered test samples and the animals were exposed for 7 successive days with same procedure. Following the 7 day period, animals were sacrificed and the transverse sections of the lung tissue were stained with Hematoxylin and Eosin (HE). Finally, the samples were visualized under light microscope for the symptoms of potential toxicity, if any.

Table 1 Concise illustration of findings of modified Ninhydrin test and enzyme assay in terms of % free amino group and % enzyme activity, respectively

S. no.	Formulation	% Free amino group	% Enzyme activity
1.	DNase-I	–	100 ± 5.2
2.	CIP-CHNPs	100 ± 4.7	–
3.	CIP-CHNPs + DNase-I	99.3 ± 2.9	97.4 ± 4.9
4.	DNase-CIP-CHNPs	39.6 ± 4.4	78.6 ± 3.8

CIP Ciprofloxacin, *DNase-I* deoxyribonuclease-I, *CIP + DNase-I* the mixture of ciprofloxacin and Deoxyribonuclease-I, *CIP-CHNPs* ciprofloxacin-loaded chitosan nanoparticles, *DNase-CIP-CHNPs* deoxyribonuclease-I functionalized ciprofloxacin-loaded chitosan nanoparticles

Table 2 Concisely summarizing the results of particle characterization

S. no.	Formulation	Characterization			
		PS ^a (nm)	PDI ^a	ZP ^a (mV)	EE ^a (%)
1.	CIP-CHNPs	196.8 ± 11.8	0.239 ± 0.05	15.3 ± 0.9	57.6 ± 4.1
2.	DNase-CIP-CHNPs	205.3 ± 8.9	0.288 ± 0.06	14.6 ± 1.3	53.7 ± 3.8

^aValue represents mean of three replicates with standard deviation (Mean ± SD)

CIP-CHNPs ciprofloxacin-loaded chitosan nanoparticles, *DNase-CIP-CHNPs* DNase-I functionalized ciprofloxacin-loaded chitosan nanoparticles

Statistical analysis

The data of antimicrobial evaluation and MTT assay were analyzed statistically by GraphPad Prism 5.0 (GraphPad Software Inc., San Diego, CA).

Results

DNase-I conjugation and enzyme activity assay

The percentage DNase-I conjugation to the chitosan nanoparticles and its relative activity (% compared to pure enzyme) were evaluated to measure the % enzyme conjugation and its hydrolytic activity, respectively. The results of evaluated parameter are summarized in Table 1. Unlike CIP-CHNPs (considered 100% amino group), DNase-CIP-CHNPs exhibited only 39.6 ± 4.4% demonstrating 66–74.8% groups were conjugated with DNase-I successfully. Meanwhile, the enzyme assay of DNase-CIP-CHNPs also demonstrated the promising enzymatic hydrolysis of the DNA (hydrolyzes around 78.6 ± 3.8% of fed DNA molecule) as compared to pure DNase-I (100% activity).

Nanof ormulation characterization (PS, PDI, ZP and %EE)

The comparative critical formulation parameters, such as PS, PDI, ZP, and %EE indicative of CIP-CHNPs and DNase-CIP-CHNPs quality are enlisted in Table 2. The findings concisely recapitulated that the quality of NPs was not compromised after the functionalization; however, a slight decrease in zeta potential was observed.

Flow property and aerodynamic property

Lower angle of repose ensures the good flow of the powder, while the higher FPF and MMAD > 1 μm make sure the desirable particle deposition in the periphery of the lungs leading to effective concentration at local site. The

DNase-CIP-CHNPs adsorbed successfully on the lactose demonstrated good flow with 31.3° ± 1.4° angle of repose. Similarly, the aerodynamic parameter such as MMAD and FPF had magnitude 40.47 ± 1.11% and 2.53 ± 0.7 μm, respectively, ensuring the considerable deposition in the lungs.

SEM analysis

Figure 1a, b is captured from SEM analysis for CIP-CHNPs and DNase-CIP-CHNPs, respectively. The SEM recorded images of NPs ensured the spherical shape and almost uniform size distribution. Measured PS was in good correlation with the size measured by particle-size analyzer. Comparative analysis of images indicated that despite the enzyme conjugation, shape and size distribution range were not affected much.

In vitro release kinetics

The relative release profile of pure CIP dispersion and CIP-CHNPs is provided in Fig. 2. Brief evaluation of release data described that precisely complete drug was displaced to the release medium from CIP dispersion within 6 h; however, the CIP-CHNPs release profile appeared to have dual release behavior. Initially, the NPs exhibited quick CIP release up

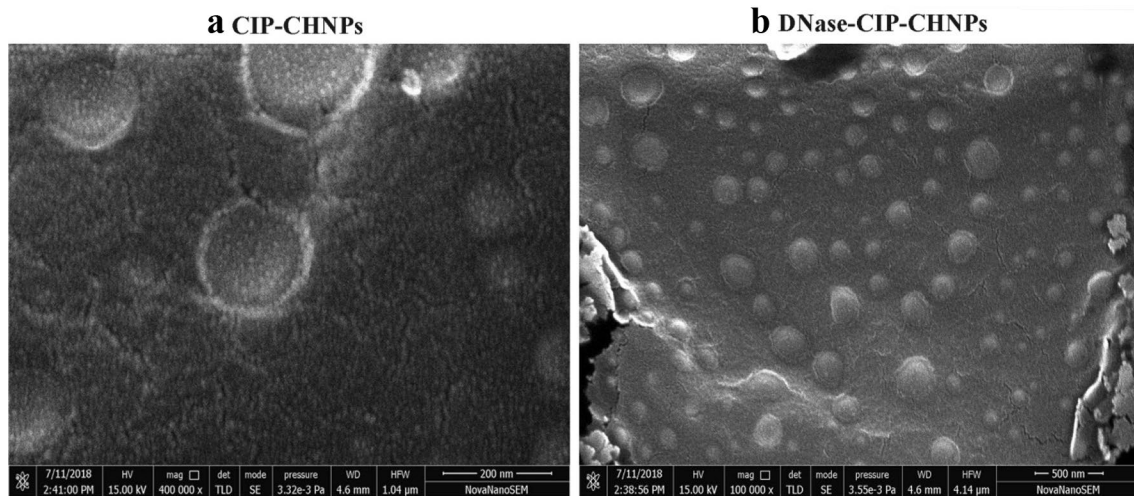


Fig. 1 SEM analysis. **a** CIP-CHNPs; **b** DNase-CIP-CHNPs

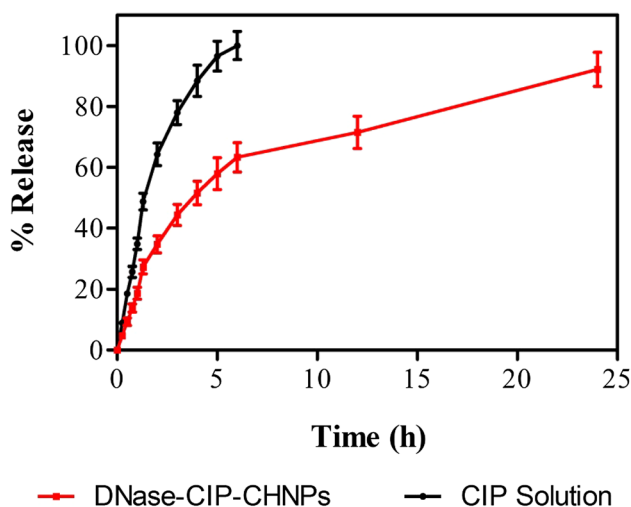


Fig. 2 In vitro release profile of nanoparticles

to $44.32 \pm 3.47\%$ in 3 h and further demonstrated slow and sustained release for next 21 h with cumulative release up to $92.19 \pm 5.57\%$. The NPs released the drug in diffusion controlled way and mimic the Higuchi release kinetics (r^2 0.936).

Minimum inhibitory concentration

Though MIC values of NPs were marginally higher compared to pure CIP (Table 3), the CIP-CHNPs rendered the overwhelming effect on susceptibility (MIC) duration against *P. aeruginosa*. The MIC of CIP after 24 h treatment was $0.0937 \mu\text{g/ml}$ and DNase-I mixing did not affect the results positively and had similar MIC value ($0.0937 \mu\text{g/ml}$). On further incubating the treated groups after 24 h,

Table 3 Antimicrobial study: brief summary of MIC and MBEC findings obtained for various treatment groups

S. no.	Formulation	MIC ($\mu\text{g/ml}$)		MBEC ($\mu\text{g/ml}$)
		24 h	48 h	24 h
1.	CIP	0.0937	0.125	3.5
2.	CIP+DNase-I	0.0937	0.125	2.25
3.	CIP-CHNPs	0.187	0.187	2.25
4.	CIP-CHNPs+DNase-I	0.187	0.187	1
5.	DNase-CIP-CHNPs	0.187	0.187	0.5

CIP Ciprofloxacin, DNase-I deoxyribonuclease-I, CIP + DNase-I the mixture of ciprofloxacin and deoxyribonuclease-I, CIP-CHNPs ciprofloxacin-loaded chitosan nanoparticles, DNase-CIP-CHNPs deoxyribonuclease-I functionalized ciprofloxacin-loaded chitosan nanoparticles

considerable bacterial growth was observed at $0.0937 \mu\text{g/ml}$ and MIC shifted to $0.125 \mu\text{g/ml}$ in CIP treatment. In contrast, CIP-CHNPs and DNase-CIP-CHNPs persuaded the convincing MIC $0.187 \mu\text{g/ml}$ after 24 h and proved to be superior in terms of preventing the microbial tolerance against drug and longer duration of action. Unlike the upshift in the MIC of pure CIP, the MIC of NPs was constant after 48 h. Moreover, the DNase-I did not possess any antimicrobial effect on tested concentration.

Minimum biofilm inhibitory concentration (MBIC)

The detailed findings of MBIC are depicted in Fig. 3a (24 h) and Fig. 3b (48 h). All the formulation prevented the biofilm adherence at $0.187 \mu\text{g/ml}$ after 24 h except CIP-CHNPs which found to have slightly higher MBIC $0.375 \mu\text{g/ml}$. At the end of 48 h, the bacteria growth was observed in CIP and CIP + DNase-I and the MBIC

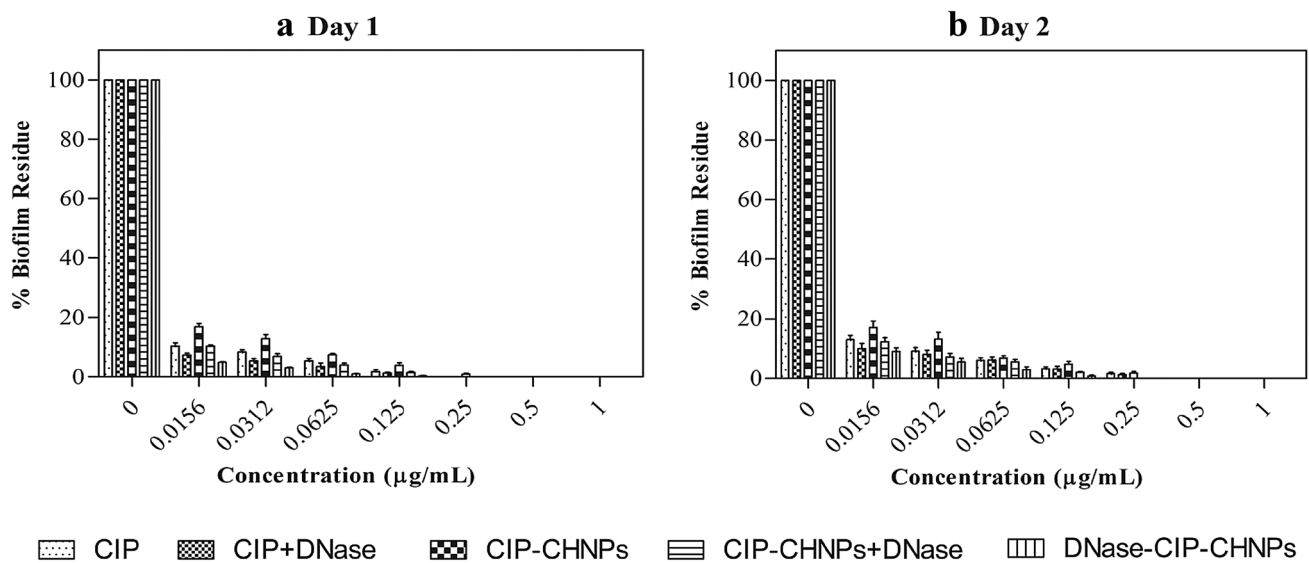


Fig. 3 Graphical illustration of minimum biofilm inhibitory concentration test where **a** and **b** correspond to the findings obtained after 24 h and 48 h, respectively

increased to 0.375 µg/ml and 0.25 µg/ml, respectively; however, the CIP-CHNPs, CIP-CHNPs + DNase-I, and DNase-CIP-CHNPs remained unaltered. At the same time, DNase-CIP-CHNPs remained the more effective treatment among all the formulation with least % biofilm adherence.

Minimum biofilm eradication concentration (MBEC)

Similar to the susceptibility data, CIP assimilation within the CHNPs along with DNase-I functionalization had rather profound effect on the biofilm matrix dispersal and eliminated microbial colonies effectively at lowest concentration. Amid all the test groups, DNase-CIP-CHNPs extensively induced the extreme biofilm dispersal competence even at minimum concentration and eliminated the biofilm completely at 0.5 µg/ml (MBEC) after 24 h incubation. However, all other treatments exhibited considerably high MBEC. The minimum concentration of pure CIP, CIP + DNase-I, CIP-CHNPs, and CIP-CHNPs + DNase-I desired to entirely confiscate the 48 h established *P. aeruginosa* biofilm was 3.5, 2.25, 2.25, and 1 µg/ml, respectively (Table 3). Furthermore, each group manifested concentration-dependent dispersal (Fig. 4a) and potentiated the biofilm elimination productivity on amalgamation of DNase-I with formulation, yet DNase-CIP-CHNPs had prompted persuasively higher biofilm dispersal and proved to be superior in comparison with other groups. Moreover, the CIP-CHNPs itself had considerably lower MBEC value as compared to the pure CIP and equivalent to CIP + DNase-I.

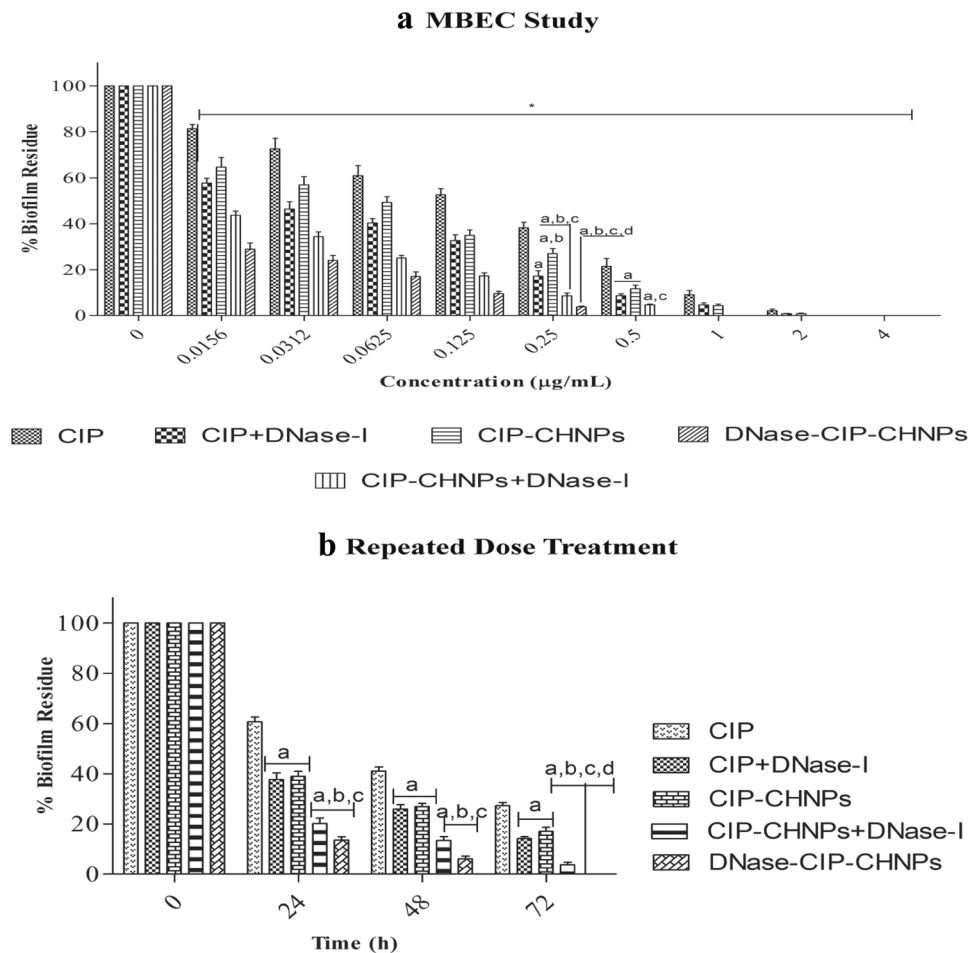
Repeated dose treatment of biofilm

Furthermore, the results of repeated dose study illustrated in Fig. 4b (0.187 µg/ml single dose/day) recapitulated the DNase-CIP-CHNPs as a superior approach to treat the biofilm *P. aeruginosa* infection in CF. Like the MBEC study, DNase-CIP-CHNPs brought about the capable and thorough elimination of the 48 h established *P. aeruginosa* biofilm on 3 days consecutive dosing at 0.187 µg/ml (equivalent to CIP). While other treatment groups failed to remove established microbial colonies in biofilm even after addition of DNase-I in 72 h treatment.

Microscopic study of biofilm

Cumulative biofilm abolition activity of DNase-CIP-CHNPs attained in MBEC and repeated dose was corroborated quantitatively and qualitatively using CLSM evaluation of untreated and treated *P. aeruginosa* biofilm (on glass cover slip). The CLSM captured z-stack fluorescent images (Fig. 5a–f) evaluated using COMSTAT 2 software to compute the biomass and thickness of biofilm (Table 4). The found outcomes were analogues to our observation during MIC and substantiated the findings of MBEC. DNase-CIP-CHNPs meritoriously contracted the biofilm-protected microbial colonies and consequently attaining the minimum biofilm thickness 13.7 ± 1.8 µm, biomass 10.8 ± 0.9 µm³/µm², and microbial density (qualitative; visually observed in CLSM images). In contrary, untreated biofilm specimen with maximum thickness 63.8 ± 2.5 µm and biomass 38.5 ± 3.4 µm³/µm² remained as a reference. Moreover, other treatment groups were not efficient enough and possess

Fig. 4 Antibiofilm study performed on 48 h established *P. aeruginosa* biofilm. **a** % biofilm residue in minimum biofilm eradication study against the tested concentration; data represented as mean \pm SD, ^a $p < 0.05$ compared to CIPR, ^b $p < 0.05$ compare to CIPR + DNase-I, ^c $p < 0.05$ compared to CIPR-CHNPs, ^d $p < 0.05$ compared to CIPR-CHNPs + DNase-I, and ^{*} $p < 0.05$ compared to 0 concentration. **b** % biofilm residue after three consecutive treatments at MIC; here, ^a $p < 0.05$ compared to CIPR, ^b $p < 0.05$ compared to CIPR + DNase-I, ^c $p < 0.05$ compared to CIPR-CHNPs, and ^d $p < 0.05$ compared to CIPR-CHNPs + DNase-I. Statistical analysis of data was done by repeated-measures two-way ANOVA



significantly ($p < 0.05$) higher biofilm thickness, biomass, and microbial density (qualitative) than DNase-CIP-CHNPs.

MTT assay

In vitro MTT testing on lungs epithelium cell line is one of the essential criteria for cytotoxicity and safety profiling of the proposed strategy (DNase-CIP-CHNPs). Data shown in Fig. 6 clearly evidenced the safety and low toxicity against the lungs epithelium cells. DNase-CIP-CHNPs along with other treatment groups had considerably high cell viability even at highest concentration tested after 24 h and almost same as untreated group.

In vivo toxicity

Lower bronchial region is characterized by its specific physiology, presence of lungs surfactant essential for gases exchange, and high susceptibility for external condition, and hence, it is regulatory mandate to evaluate the drug delivery safety proposed for the pulmonary route. In this regard, various treatment groups were tested histologically to evaluate the possible toxicity on lung tissues in vivo. The

microscopically assessed HE stained images of lungs tissue following different treatments (Fig. 7a–f) strongly favor the safety of the proposed strategy for pulmonary route administration.

Discussion

Biofilm production is an intrinsic behavior of microbes to protect them from host body environment by shielding the colonies within self-secreted ECM. Likewise, *P. aeruginosa* extensively secretes the matrix in various body infection and contribute in the disease progression and chronicity. Specifically, in cystic fibrosis, *P. aeruginosa* biofilm facilitate the disease complication, antibiotic resistance, and accountable for the high rate of morbidity and mortality (Kidd et al. 2018). Several studies has already reported the potential use of DNase-I in conjunction with antibiotics or alone to cleave the eDNA in biofilm to improve the antimicrobial susceptibility (Alipour et al. 2009; Tetz and Tetz 2010; Kaplan et al. 2012) and has been proved to be safe and compatible in vivo (Shah et al. 1996). Therefore, the current study highlighted the development of the formulation with

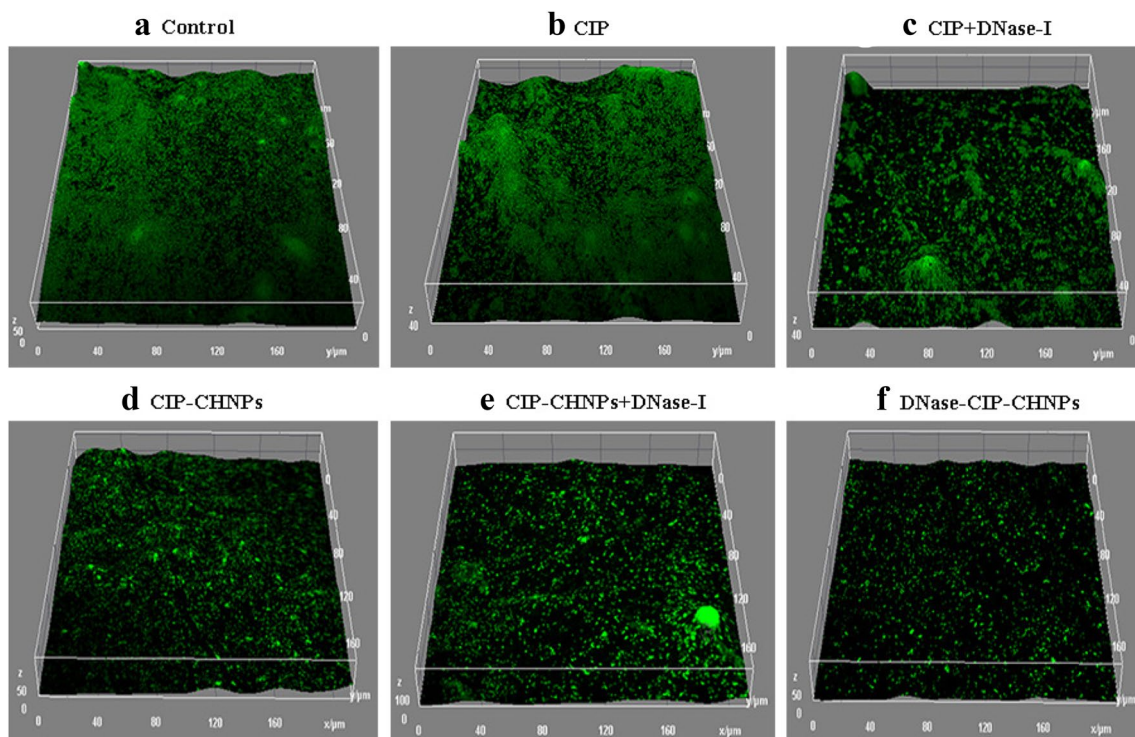


Fig. 5 Confocal images of *P. aeruginosa* biofilm treated with tests groups including control (a), CIP (b), CIP+DNase-I (c), CIP-CHNPs (d), CIP-CHNPs + DNase-I (e), and DNase-CIP-CHNPs (f)

Table 4 Brief summary of thickness and biomass of biofilms treated with mentioned groups

Treatment	Biofilm parameters (Mean \pm SD)	
	Thickness (μm)	Biomass ($\mu\text{m}^3/\mu\text{m}^2$)
Control (untreated)	63.8 \pm 2.5	38.5 \pm 3.4
CIP	51.9 \pm 4.7	28.4 \pm 3.2
CIP+DNase-I	39.1 \pm 3.2	22.8 \pm 2.1
CIP-CHNPs	35.2 \pm 3.4	25.7 \pm 1.8
CIP-CHNPs + DNase-I	23.6 \pm 2.1	16.4 \pm 1.7
DNase-CIP-CHNPs	13.7 \pm 1.8 ^a	10.8 \pm 0.9 ^a

^aSignificant difference of DNase-CIP-CHNPs treatment vs respective groups ($p < 0.05$; one-way ANOVA; Mean \pm SD; $n = 3$)

potential to improve the antibiotics distribution in biofilm by hydrolyzing the eDNA a prominent component of ECM, consequently reducing the resistance and improving the bacterial exposure for antibiotics effectively keeping the lung's physiological condition unaffected. Therefore, ciprofloxacin-loaded chitosan nanoparticles functionalized with DNase-I were optimized. DNase-I disperse the biofilm matrix by hydrolyzing the eDNA, while the chitosan NPs improve the biofilm penetration and release the drug in controlled fashion in close vicinity of microbial colonies.

CIP-CHNPs formulated using the ionotropic gelation method had characteristics ideal for the biofilm penetration and treatment. After that, the DNase-I was successfully attached covalently (amide) to the amino group of chitosan using the carbodiimide chemistry (Hou et al. 2017). Besides 66–74.8% (39.6 \pm 4.4% free amino) conjugation evaluated using modified Ninhydrin test, DNase-CIP-CHNPs demonstrated exceptionally higher hydrolytic efficacy against (78.6 \pm 3.8%) the eDNA compared to the pure DNase-I. After conjugation, DNase-CIP-CHNPs shown to had almost analogous PS, PDI, ZP and %EE to CIP-CHNPs and were unaltered. Hydrophilic nature of CIP was an fundamental cause of low %EE (Bilati et al. 2005), even though the attained particle characteristics were satisfactory to claim it as a stable formulation and adequate for the effective treatment of biofilm *P. aeruginosa* infection in CF. The particles with such small diameter can easily penetrate the thick mucus filled in CF patients lungs (Suk et al. 2009) and thereby expedite the drug distribution in the biofilm. In addition, the SEM images of CIP-CHNPs and DNase-CIP-CHNPs (Fig. 1) had spherical shape, smoother surface, and smaller particle diameter than measured by zeta sizer, and could be attributed to the obvious reason of measuring hydrodynamic diameter by zeta sizer.

Enzymes (DNase-I) being thermosensitive and denatured or lose their activity on higher temperature; hence,

Fig. 6 In vitro toxicity data performed on lungs epithelium cell line. Two-way ANOVA was performed to evaluate the toxicity data statistically (here data represent the mean \pm SD and $p > 0.05$ considered as insignificant; other groups vs DNase-CIP-CHNPs)

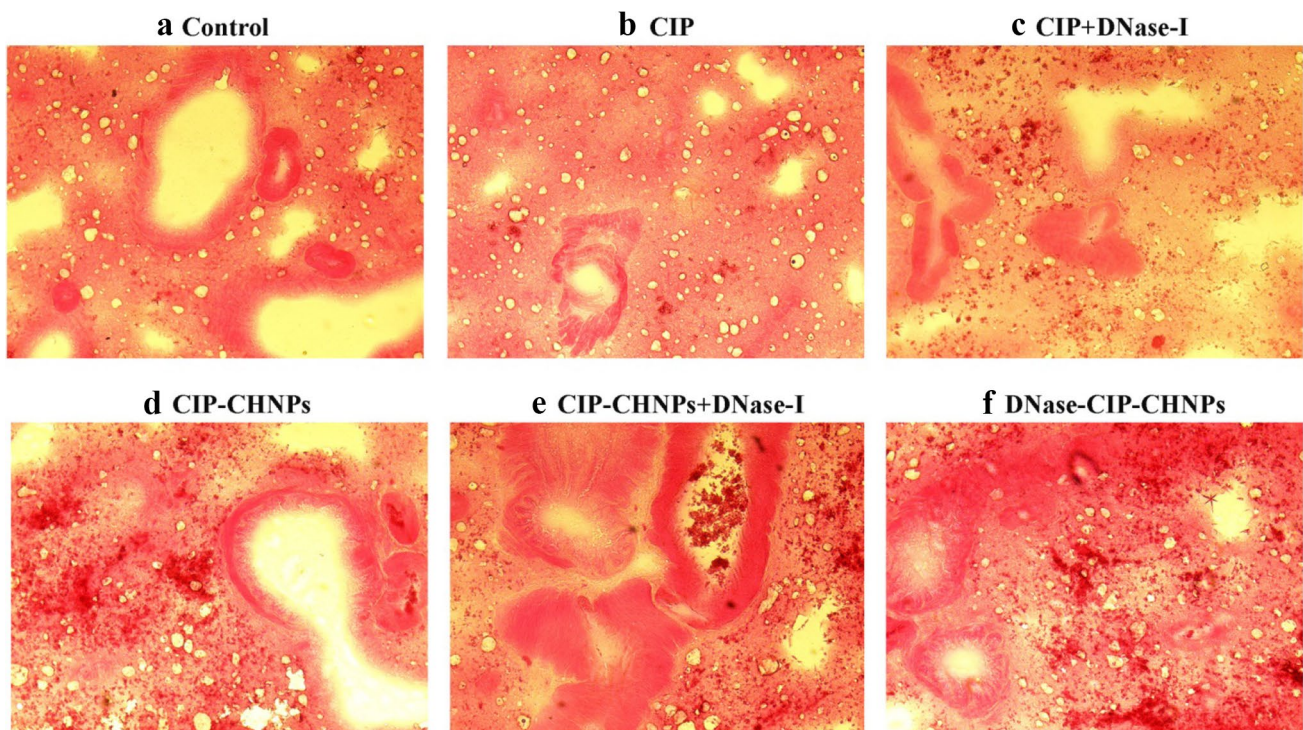
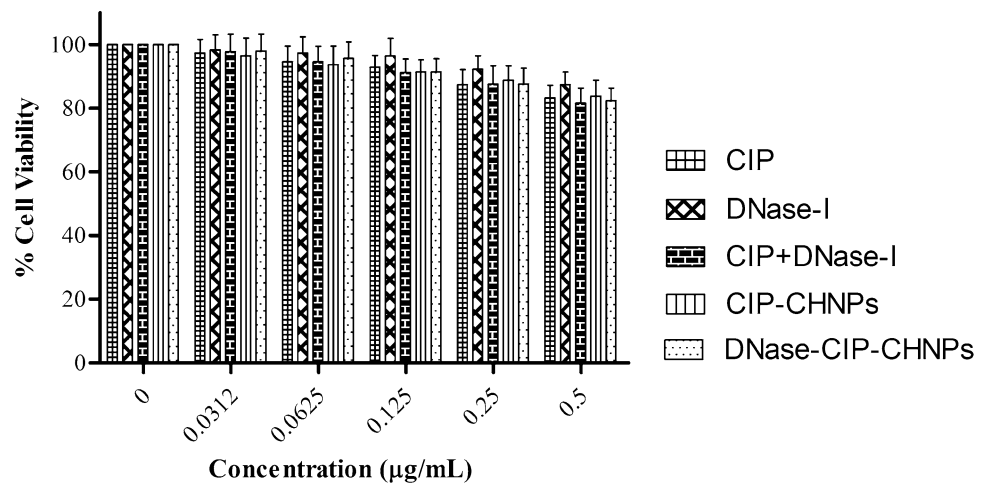


Fig. 7 In vivo toxicity data: rat lung's histological images obtained after exposing with various formulations revealing the possible toxicity

nanoparticles were powdered using three-step freeze drying process with the help of lactose (cryoprotectant). Furthermore, pulmonary delivery requisite distinct properties to achieve the desired particle deposition in the lungs, and hence, the freeze-dried NPs were adsorbed on the fine-grade lactose powder to incorporate stability and ideal inhalable properties. The lactose adsorbed NPs performed well and gave acceptable range of MMAD $2.53 \pm 07 \mu\text{m}$ and FPF $40.47 \pm 1.11\%$ appropriate for inhalation and attaining the enough lung deposition. Moreover, it possesses good flow property, as indicated by angle of repose, which signify easy

flow of powder, while optimum in vitro aerodynamic property (such as FPF and MMAD) confirms the adequate lung deposition of particles to attain the sufficient concentration required for biofilm dispersal and local targeting with better stability.

In the in vitro release study, DNase-CIP-CHNPs demonstrated time-dependent release profile (Fig. 2). Initially, the surface bound drug contributed the burst release during the initial hours followed by slow diffusion of molecularly distributed CIP from chitosan matrix correspond to the controlled release up to 24 h. The initial burst release achieves

the necessary loading dose and short onset of action effectively. In contrast, the slow diffusion of drug from chitosan NPs maintains the MIC and thus has advantages over conventional drug delivery (Cheow et al. 2010). Altogether, such release profile has worthwhile an effect on the antimicrobial activity thus brings about the accelerated and potentiated antimicrobial activity of drug which effectually averts the microbial biofilm resistance against the antimicrobial therapy.

In addition, the CIP-CHNPs and DNase-CIP-CHNPs established the exemplary conclusion on in vitro antimicrobial testing. After 24 h, the CIP-CHNPs, and DNase-CIP-CHNPs inhibited the bacterial growth at the MIC 0.187 µg/ml, whereas the CIP had 0.0937 µg/ml MIC. Although, NPs had higher MIC compared to the pure CIP after 24 h, but after 48 h, NPs activity was consistent and had constant MIC; however, the CIP-treated group exhibited the extensive microbial growth in the media and the MIC shifted to 0.125 µg/ml. These findings recapitulated that single dose of NPs was sufficient enough to competently prolong the microbial inhibition and avert the chance of microbial resistance. Interestingly, unique NPs aspects such as facilitated NPs adhesion to microbial cell, prevention of steric resistance, and release pattern easily interpreted the findings of MIC, wherein burst release fulfilled the desired loading dose; however, the slow and sustained release maintained the MIC for longer duration and thus circumvented the possibility of microbial growth (Wang et al. 2017). Achieving the sublethal concentration may initiate the microbial tolerance and resistance to antibiotics therapy (Jørgensen et al. 2013). Meanwhile, MBIC, a minimum concentration of antibiotics that avoid the surface attachment planktonic bacterial and thereby inhibit biofilm development, was studied. Interestingly, the findings of MBIC were promising and supported the MIC results. Interestingly, NPs had prolonged antimicrobial activity up to 48 h compared to CIP alone and exhibited no sign microbial growth in the culture on day 2 on the same concentration (48 h). However, the CIP was efficiently able to prevent the biofilm growth on day 1 (24 h), but exhibited the considerable microbial or biofilm formation after 48 h. Aspects such as higher penetration efficiency of NPs in mucin that accelerate drug dispersion within biofilm, higher cell adhesion, and control release of drug for longer duration in close vicinity of microbial colony prevent the microbial tolerance (Cheow et al. 2010; Al-Nemrawi et al. 2018). Moreover, the presence of DNase-I within the NPs averted the microbial surface adhesion and biofilm production which used to degrade the eDNA and obviated the biofilm growth (Kaplan et al. 2012; Okshevsky et al. 2015). Among all the formulations, DNase-CIP-CHNPs demonstrated the highest intrinsic potential to avoid the biofilm growth in planktonic bacterial suspension. Furthermore, a minimum concentration anticipated for total elimination of established biofilm

efficiently called MBEC was evaluated. The DNase-CIP-CHNPs performed remarkably well in MBEC assay and completely disperse the 48 h established biofilm of *P. aeruginosa* after 24 h treatment at 0.5 µg/ml concentration, however; all other formulation depleted the biofilm at higher concentration (Table 3). Though all the treatment groups dismantle the biofilm in concentration-dependent manner, still the DNase-CIP-CHNPs alone evidenced the highest antimicrobial activity and entirely removed the microbial cell from biofilm effectively (Fig. 4a) at lowest concentration (MBEC 0.5 µg/ml). Interestingly, CIP-CHNPs and CIPR + DNase-I rendered the similar antibiofilm profile but more effective than CIP which has least antibiofilm activity and maximum MBEC (Fig. 4a). The least antibiofilm activity of CIP and formulation other than DNase-CIP-CHNPs may be assigned to the higher resistance enforced by biofilm matrix due to compromised mobility and penetrability (Tré-Hardy et al. 2008; Van Acker et al. 2014). On the other hand, DNase-I considerably augmented the activity of NPs and CIP against the biofilm by hydrolyzing the eDNA and thus amplified the penetration, mobility, and distribution (Kaplan et al. 2012; Baelo et al. 2015), and it also inhibits the microbial surface adhesion and prevents the biofilm growth formation (Okshevsky et al. 2015). Thereby, DNase-I favors the accumulation of CIP and NPs deep inside the biofilm in vicinity of the microbial colonies and enhancement of microbial susceptibility within biofilm for drug.

In addition, 48 h established biofilm was repeatedly treated with three consecutive doses (at MIC 0.187 µg/ml) to support the above antimicrobial results. Unlike other treatments, DNase-CIP-CHNPs had rather highest activity and entirely depleted biofilm after three consecutive dosing during 72 h. Comprehensive analysis and data extraction in terms of biofilm thickness and biomass by processing of confocal images also substantially supported the MBEC. The DNase-I significantly reduced the microbial count (green fluorescent density in CLSM images), thickness, and biomass in combination with CIP and NPs. The CIP alone revealed very little antibiofilm potential compared to control and can be seen clearly in the Fig. 5b where the CIP had intense green fluorescence similar to control (Fig. 5a) confirming the presence of high-density live *P. aeruginosa* cell in biofilm. At the same time, CIP along with DNase-I (Fig. 5c) decreased the bacterial density significantly. Similarly, the CIP-CHNPs + DNase-I had higher live cell density (Fig. 5d) compared to CIP-CHNPs alone (Fig. 5e). Among all the treatments, the DNase-CIP-CHNPs in Fig. 5f evidenced the most efficient biofilm dispersal and had least cell density, thickness, and biomass of biofilm. Hence, the incorporation of DNase-I in formulation augmented the antimicrobial potential of formulation by disturbing the favorable and complex living habitat (Biofilm) of bacteria. These augmented activities corresponded to eDNA degradation

in biofilm by DNase-I hydrolytic activity. However, nanoparticles incorporated the higher biofilm penetrability and controlled drug release to the formulation. Concisely, the data in hands from antimicrobial studies cumulatively support that CIP-CHNPs significantly prolonged the duration of MIC and reduced the MBEC. Similarly, the incorporation of DNase-I along with NPs and CIP also improved the antimicrobial efficacy against the biofilm-protected *P. aeruginosa* colonies.

Finally, the in vitro and in vivo studies were conducted to identify the severe toxicity on the lungs epithelium cell line and animal lungs, respectively. Succinctly, none of the formulation had induced the significant toxicity on the cell line and microstructure of the lungs. Hence, it is found to be safe and effective for the pulmonary delivery.

Conclusion

The proposed nanoparticles were successfully developed and proved to have unprecedented antimicrobial potential against the planktonic (MIC) and biofilm (MBEC) shielded *P. aeruginosa* both. Moreover, the CLSM image examination also ascertained that DNase-CIP-CHNPs maximally reduced the microbial count, biomass, and thickness of established *P. aeruginosa* biofilm. The empirically collected data from various studies were encouraging and cumulatively re-assuring that DNase-I functionalized CIP-CHNPs have the enormous potential to inhibit biofilm development and break the previously established biofilm ECM, which consequently improve the antimicrobial activity of CIP against the biofilm surrounded *P. aeruginosa* without triggering the severe lung toxicity. Thus, the findings of this study recommended that, DNase-CIP-CHNPs can be an safe and effective alternative approach to treat the *P. aeruginosa* biofilm infection in the cystic fibrosis.

Acknowledgements The authors are grateful to Indian Institute of Technology (Banaras Hindu University), Varanasi, for rendering the support in terms of infrastructure, facilities, and research support grant to complete the work on time. We also thank the Central Instrument Facility Centre, IIT (BHU), Varanasi for extending the facilities when needed. We also acknowledge the Interdisciplinary school of life sciences, Institute of Science, Banaras Hindu University, Varanasi for confocal microscopy. Moreover, we are also thankful to Ministry of Human Resources and Development, Government of India for offering Mr. K.K. Patel teaching assistantship to complete his Ph.D.

Compliance with ethical standards

Conflict of interest Authors have no conflict of interest.

References

- Agrawal AK, Harde H, Thanki K, Jain S (2013) Improved stability and antidiabetic potential of insulin containing folic acid functionalized polymer stabilized multilayered liposomes following oral administration. *Biomacromol* 15(1):350–360
- Agrawal AK, Urimi D, Harde H, Kushwah V, Jain S (2015) Folate appended chitosan nanoparticles augment the stability, bioavailability and efficacy of insulin in diabetic rats following oral administration. *RSC Adv* 5(127):105179–105193
- Agrawal AK, Aqil F, Jeyabalan J, Spencer WA, Beck J, Gachuki BW, Alhakeem SS, Oben K, Munagala R, Bondada S (2017a) Milk-derived exosomes for oral delivery of paclitaxel. *Nanomed Biol Med* 13(5):1627–1636
- Agrawal AK, Kumar K, Swarnakar NK, Kushwah V, Jain S (2017b) “Liquid crystalline nanoparticles”: rationally designed vehicle to improve stability and therapeutic efficacy of insulin following oral administration. *Mol Pharm* 14(6):1874–1882
- Algburi A, Comito N, Kashtanov D, Dicks LMT, Chikindas ML (2017) Control of biofilm formation: antibiotics and beyond. *Appl Environ Microbiol* 83(3):e02508–e02516
- Alipour M, Suntres ZE, Omri A (2009) Importance of DNase and alginate lyase for enhancing free and liposome encapsulated aminoglycoside activity against *Pseudomonas aeruginosa*. *J Antimicrob Chemother* 64(2):317–325
- Al-Nemrawi N, Alshraideh NA, Zayed A, Altaani B (2018) Low molecular weight chitosan-coated PLGA nanoparticles for pulmonary delivery of tobramycin for cystic fibrosis. *Pharmaceuticals* 11(1):28
- Aqil F, Munagala R, Jeyabalan J, Agrawal AK, Gupta R (2017) Exosomes for the enhanced tissue bioavailability and efficacy of curcumin. *AAPS J* 19(6):1691–1702
- Baelo A, Levato R, Julián E, Crespo A, Astola J, Gavaldà J, Engel E, Mateos-Timoneda MA, Torrents E (2015) Disassembling bacterial extracellular matrix with DNase-coated nanoparticles to enhance antibiotic delivery in biofilm infections. *J Control Release* 209:150–158
- Bilati U, Allémann E, Doelker E (2005) Development of a nanoprecipitation method intended for the entrapment of hydrophilic drugs into nanoparticles. *Eur J Pharm Sci* 24(1):67–75
- Cheow WS, Chang MW, Hadinoto K (2010) Antibacterial efficacy of inhalable levofloxacin-loaded polymeric nanoparticles against *E. coli* biofilm cells: the effect of antibiotic release profile. *Pharm Res* 27(8):1597–1609
- Chiang W-C, Nilsson M, Jensen PØ, Højby N, Nielsen TE, Givskov M, Tolker-Nielsen T (2013) Extracellular DNA shields against aminoglycosides in *Pseudomonas aeruginosa* biofilms. *Antimicrob Agents Chemother* 57(5):2352–2361
- Cutting K, Percival S, Williams D (2009) Biofilms: possible strategies for suppression in chronic wounds. *Nurs Stand* 23(32):64–72
- Del Pozo J, Patel R (2007) The challenge of treating biofilm-associated bacterial infections. *Clin Pharmacol Ther* 82(2):204–209
- Forier K, Raemdonck K, De Smedt SC, Demeester J, Coenye T, Braeckmans K (2014) Lipid and polymer nanoparticles for drug delivery to bacterial biofilms. *J Control Release* 190:607–623
- Harde H, Agrawal AK, Jain S (2014) Development of stabilized glucosaminosylated chitosan nanoparticles using tandem crosslinking method for oral vaccine delivery. *Nanomedicine* 9(16):2511–2529
- Hou J, Yu X, Shen Y, Shi Y, Su C, Zhao L (2017) Triphenyl phosphine-functionalized chitosan nanoparticles enhanced antitumor efficiency through targeted delivery of doxorubicin to mitochondria. *Nanoscale Res Lett* 12(1):158
- Jain S, Patil SR, Swarnakar NK, Agrawal AK (2012) Oral delivery of doxorubicin using novel polyelectrolyte-stabilized liposomes (layersomes). *Mol Pharm* 9(9):2626–2635

- Jain S, Spandana G, Agrawal AK, Kushwah V, Thanki K (2015) Enhanced antitumor efficacy and reduced toxicity of docetaxel loaded estradiol functionalized stealth polymeric nanoparticles. *Mol Pharm* 12(11):3871–3884
- Jørgensen KM, Wassermann T, Jensen PØ, Hengzuang W, Molin S, Høiby N, Ciofu O (2013) Sublethal ciprofloxacin treatment leads to rapid development of high-level ciprofloxacin resistance during long-term experimental evolution of *Pseudomonas aeruginosa*. *Antimicrob Agents Chemother* 57(9):4215–4221
- Juárez-Morales L, Hernandez-Cocolezti H, Chigo-Anota E, Aguila-Almanza E, Tenorio-Arvide M (2017) Chitosan-aflatoxins B1, M1 interaction: a computational approach. *Curr Org Chem* 21(28):2877–2883
- Kaplan JB, LoVetri K, Cardona ST, Madhyastha S, Sadovskaya I, Jabbouri S, Izano EA (2012) Recombinant human DNase I decreases biofilm and increases antimicrobial susceptibility in staphylococci. *J Antibiot* 65(2):73
- Kidd TJ, Canton R, Ekkelenkamp M, Johansen HK, Gilligan P, LiPuma JJ, Bell SC, Elborn JS, Flume PA, VanDevanter DR (2018) Defining antimicrobial resistance in cystic fibrosis. *J Cystic Fibros*. <https://doi.org/10.1016/j.jcf.2018.08.014>
- Kushwah V, Agrawal AK, Dora CP, Mallinson D, Lamprou DA, Gupta RC, Jain S (2017) Novel gemcitabine conjugated albumin nanoparticles: a potential strategy to enhance drug efficacy in pancreatic cancer treatment. *Pharm Res* 34(11):2295–2311
- Kushwah V, Katiyar SS, Dora CP, Agrawal AK, Lamprou DA, Gupta RC, Jain S (2018) Co-delivery of docetaxel and gemcitabine by anacardic acid modified self-assembled albumin nanoparticles for effective breast cancer management. *Acta Biomater* 73:424–436
- Mu H, Tang J, Liu Q, Sun C, Wang T, Duan J (2016) Potent antibacterial nanoparticles against biofilm and intracellular bacteria. *Sci Rep* 6:18877
- Muttill P, Kaur J, Kumar K, Yadav AB, Sharma R, Misra A (2007) Inhalable microparticles containing large payload of anti-tuberculosis drugs. *Eur J Pharm Sci* 32(2):140–150
- Okshevsky M, Regina VR, Meyer RL (2015) Extracellular DNA as a target for biofilm control. *Curr Opin Biotechnol* 33:73–80
- Oliver A, Cantón R, Campo P, Baquero F, Blázquez J (2000) High frequency of hypermutable *Pseudomonas aeruginosa* in cystic fibrosis lung infection. *Science* 288(5469):1251–1253
- Pang Z, Raudonis R, Glick BR, Lin TJ, Cheng Z (2019) Antibiotic resistance in *Pseudomonas aeruginosa*: mechanisms and alternative therapeutic strategies. *Biotechnol Adv* 37(1):177–192
- Patel KK, Gade S, Anjum MM, Singh SK, Maiti P, Agrawal AK, Singh S (2019a) Effect of penetration enhancers and amorphization on transdermal permeation flux of raloxifene-encapsulated solid lipid nanoparticles: an ex vivo study on human skin. *Appl Nanosci*. <https://doi.org/10.1007/s13204-019-01004-6>
- Patel KK, Surekha DB, Tripathi M, Anjum MM, Muthu M, Tilak R, Agrawal AK, Singh S (2019b) Anti-biofilm potential of silver sulfadiazine loaded nanoparticle formulations: a study on the role of DNase-I in microbial biofilm and wound healing activity. *Mol Pharm*. <https://doi.org/10.1021/acs.molpharmaceut.9b00527>
- Prochazkova S, Vårum KM, Ostgaard K (1999) Quantitative determination of chitosans by ninhydrin. *Carbohydr Polym* 38(2):115–122
- Ramos MADS, Da Silva PB, Sposito L, De Toledo LG, Bonifacio BV, Rodero CF, Dos Santos KC, Chorilli M, Bauab TM (2018) Nanotechnology-based drug delivery systems for control of microbial biofilms: a review. *Int J Nanomed* 13:1179
- Rybtke TM, Jensen PO, Hoiby N, Givskov M, Tolker-Nielsen T, Bjarnsholt T (2011) The implication of *Pseudomonas aeruginosa* biofilms in infections. *Inflamm Allergy-Drug Targets (Formerly Curr Drug Targets Inflamm Allergy)* 10(2):141–157
- Sauer K, Camper AK, Ehrlich GD, Costerton JW, Davies DG (2002) *Pseudomonas aeruginosa* displays multiple phenotypes during development as a biofilm. *J Bacteriol* 184(4):1140–1154
- Shah PL, Scott SF, Knight RA, Marriott C, Ranasinha C, Hodson ME (1996) In vivo effects of recombinant human DNase I on sputum in patients with cystic fibrosis. *Thorax* 51(2):119–125
- Suk JS, Lai SK, Wang Y-Y, Ensign LM, Zeitlin PL, Boyle MP, Hanes J (2009) The penetration of fresh undiluted sputum expectorated by cystic fibrosis patients by non-adhesive polymer nanoparticles. *Biomaterials* 30(13):2591–2597
- Tetz VV, Tetz GV (2010) Effect of extracellular DNA destruction by DNase I on characteristics of forming biofilms. *DNA Cell Biol* 29(8):399–405
- Tré-Hardy M, Vanderbist F, Traore H, Devleeschouwer MJ (2008) In vitro activity of antibiotic combinations against *Pseudomonas aeruginosa* biofilm and planktonic cultures. *Int J Antimicrob Agents* 31(4):329–336
- Urmi D, Agrawal AK, Kushwah V, Jain S (2019) Polyglutamic acid functionalization of chitosan nanoparticles enhances the therapeutic efficacy of insulin following oral administration. *AAPS PharmSciTech* 20(3):131
- Van Acker H, Van Dijck P, Coenye T (2014) Molecular mechanisms of antimicrobial tolerance and resistance in bacterial and fungal biofilms. *Trends Microbiol* 22(6):326–333
- Wang L, Hu C, Shao L (2017) The antimicrobial activity of nanoparticles: present situation and prospects for the future. *Int J Nanomed* 12:1227
- Whitchurch CB, Tolker-Nielsen T, Ragas PC, Mattick JS (2002) Extracellular DNA required for bacterial biofilm formation. *Science* 295(5559):1487
- Wu H, Moser C, Wang H-Z, Høiby N, Song Z-J (2015) Strategies for combating bacterial biofilm infections. *Int J Oral Sci* 7(1):1
- Yang Y, Bajaj N, Xu P, Ohn K, Tsifansky MD, Yeo Y (2009) Development of highly porous large PLGA microparticles for pulmonary drug delivery. *Biomaterials* 30(10):1947–1953